Available online at www.sciencedirect.com
ScienceDirect
Polymer 47 (2006) 8556–8561
polymer
www.elsevier.com/locate/polymer

Reinforcement of polymers with carbon nanotubes. The role of an ordered polymer interfacial region. Experiment and modeling

Jonathan N. Coleman [a,*], Martin Cadek [a], Kevin P. Ryan [a], Antonio Fonseca [b], Janos B. Nagy [b], Werner J. Blau [a], Mauro S. Ferreira [a]

[a] *School of Physics, Trinity College Dublin, Dublin 2, Ireland*
[b] *Laboratoire de Résonance Magnétique Nucléaire, FUNDP, 61 Rue de Bruxelles, 5000 Namur, Belgium*

Received 25 April 2006; accepted 16 October 2006
Available online 2 November 2006

Abstract

Significant increases in the Young's modulus of nanotube–polymer composites have been associated with the formation of an ordered polymer layer coating the nanotubes. Polyvinyl alcohol (PVA) is known to display nanotube-induced ordering. It is used here as a model matrix to investigate how the polymer coating influences the mechanical reinforcement of the composite material. Young's modulus and calorimetry measurements were carried out on films of PVA-based composites reinforced with different types of nanotubes. An unmistakable correlation between polymer ordering and reinforcement was found. This is supported by the introduction of a model capable of establishing, on quantitative grounds, how the ordered phase affects the increase in the Young's modulus. Rather than acting as intrinsically stiffer reinforcing agents, our results suggest that the major role played by the nanotubes in improving the mechanical properties of composites is to nucleate an ordered polymer coating. It is the presence of this stiff ordered phase that dominates the reinforcement mechanism.

Keywords: Carbon nanotubes; Polyvinyl alcohol; Young's modulus

Carbon nanotubes are among the stiffest [1] and strongest [2,3] materials known to mankind. For this reason and due to their relatively low density and high aspect ratio, they have been suggested as ideal fillers for the mechanical reinforcement of plastics. However, results have been somewhat disappointing, as only few papers [30] have reported levels of reinforcement matching those predicted by models such as the rule of mixtures [4].

Paradoxically, some excellent results have been attained, where the reinforcement *exceeds* the maximum predicted by the rule of mixtures. These cases are connected by one common factor: the use of polyvinyl alcohol as the matrix material [5–9]. Moreover, most of these papers report enhanced polymer crystallinity in the composite relative to the pure polymer [5–8]. This is observed as a melt peak in differential scanning calorimetry measurements. It has been suggested that polymer crystallization is nucleated on the surface of nanotubes during film drying. This is confirmed by microscopic investigations of fractured film surfaces showing thick polymer coatings still covering the nanotubes after fracture [8]. While it is unlikely that this interfacial phase is a true polymer crystal, it is certainly ordered relative to the amorphous polymer phase.

Whereas the correlation between this ordered polymer phase and mechanical reinforcement is evident, the actual role played by an ordered interfacial phase on the reinforcement of these composites is still unclear. On the one hand, such a layer may improve stress transfer between the polymer and the nanotube through a more ordered interface between these two phases. On the other hand, the ordered phase is likely to be intrinsically stiffer than its amorphous counterpart, leading to some degree of reinforcement. The goal of this communication is to identify if and how these two mechanisms affect the

* Corresponding author.
E-mail address: colemaj@tcd.ie (J.N. Coleman).

0032-3861/$ - see front matter © 2006 Elsevier Ltd. All rights reserved.
doi:10.1016/j.polymer.2006.10.014

reinforcement. Ideally, one would also wish to quantify their respective contributions to the mechanical reinforcement, thus determining the dominant mechanism and potentially establishing the best procedures for further enhancement of their mechanical properties.

With this motivation, in this work we fabricate composites from polyvinyl alcohol and a range of nanotube types. Both mechanical and thermal measurements have been carried out to study the effect of the nanotubes on both Young's modulus and crystallinity. The nanotubes used were double walled nanotubes (DWNT) from Nanocyl S.A. (Belgium)[1], arc grown MWNT [10] produced in our own laboratory (Arc-MWNT), two types of catalytic MWNT from Nanocyl S.A. (CVD-1, CVD-2)[1], and catalytic MWNT produced in Orléans (France) [11] (CVD-3). In all cases except Arc-MWNT, the nanotubes were pure when received. For Arc-MWNT the NT material was purified during the composite formation process [5].

A range of composite dispersions was prepared for each nanotube type by adding the nanotube material to 30 g/l solutions of PVA in water. PVA ($M_w = (30K-70K)$ g/mol) used in this investigation was purchased from Sigma–Aldrich [product code: 9002-89-5] and used as supplied. In case of Arc-MWNT a mass fraction of 25% soot relative to the polymer content was added to the polymer solution. This solution was mixed and purified as described previously [5] and the true nanotube mass fraction was measured by thermal gravimetric analysis. For all other nanotube types, the maximum mass fraction added to the polymer solution was 1 wt%. These samples were sonicated for 5 min using a high power sonic tip followed by a mild sonification for 2 h followed by further high power sonification for additional 5 min.

To fabricate free-standing composite films, 1 ml of each solution was pipetted onto a polished Teflon disk and placed in a 60 °C heated oven to allow evaporation of the solvent. This procedure was repeated four times on each disk in order to obtain films with thicknesses of up to 0.3 mm. The films were peeled off the substrates and cut into strips of ~10 mm × 4 mm × 0.3 mm to perform mechanical testing. Prior to testing, all specimens underwent an additional drying procedure for 1 h at 60 °C to evaporate any remaining water. It should be pointed out that great care must be taken to ensure that all films receive similar exposure to ambient conditions prior to testing. Otherwise large variations in adsorbed water content result in large variations in mechanical properties. The width and thickness of each strip were measured using a low torque digital micrometer. The volume fraction of NT in each film was calculated from the mass fraction using the densities, $\rho = 1300$ kg/m^3 for PVA, $\rho = 1500$ kg/m^3 for DWNT and $\rho = 2150$ kg/m^3 for all MWNT.

In order to measure the average diameter and length of each nanotube type, transmission electron microscopy was performed (Hitachi H-7000). Formvar coated copper grids (mesh size 300) were dipped into composite solutions and allowed to dry in ambient conditions. The average diameter, D, and length, l, of each type of nanotube were found to be DWNT: $D = 2.5$ nm, $l \sim 2.2$ μm; CVD-1: $D = 15$ nm, $l \sim 1.8$ μm; CVD-2: $D = 14$ nm, $l \sim 2.1$ μm; CVD-3: $D = 16$ nm, $l \sim 3.8$ μm; Arc-MWNT: $D = 24$ nm, $l \sim 1$ μm.

Tensile testing was carried out using a Zwick Z100 tensile tester. A 100 N load cell and a cross head speed of 0.5 mm/min were used to obtain the Young's modulus, Y. In all cases four strips were measured and the mean and standard deviation calculated. Furthermore, morphology and thermal properties of the composites were studied by differential scanning calorimetry (DSC) using a Perkin–Elmer Diamond DSC power compensation instrument. Scanning rate was 40 K/min where approximately 10 mg of each sample was measured and analyzed.

Stress (σ)–strain (ε) measurements (not shown) were made for all composite types and all volume fractions. In all cases the curves were linear at low strain followed by plastic deformation in the region of 3% strain. At higher strains the films yield up to a breaking strain of 6% for the pure polymer. In general the curves were similar in form to those depicted in figure 5 of Ref. [8]. Values for Young's modulus were measured from $d\sigma/d\varepsilon$ at low strain. These are plotted as a function of nanotube volume fraction for all composite types in Fig. 1. The Young's modulus for the pure polymer was $Y = 1.9 \pm 0.3$ GPa. In all cases the modulus increased linearly with volume fraction at low volume fraction. In most cases this linearity was observed over the entire volume fraction range. However, in the case of CVD-3 and DWNT-based samples the modulus tended to saturate and even decrease with volume fraction at higher volume fractions. This is due to nanotube aggregation effects that can occur even at low volume fraction, especially in the case of catalytic MWNT [12] and both SWNT [6] and DWNT [6]. Nanotube aggregation has previously been observed to cause a reduction in both modulus and strength as volume fraction is increased [12]. In all cases the modulus enhancement can be characterized by the slope (dY/dV_f) of the Y–V_f curve measured at low V_f. These values are given in Table 1.

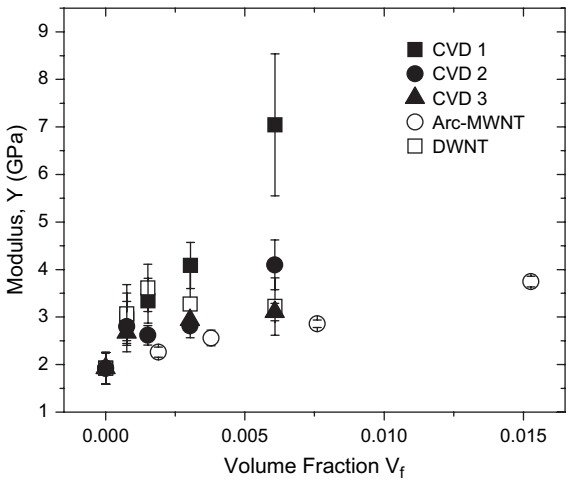

Fig. 1. Young's modulus as a function of nanotube volume fraction for all tube types in PVA matrices.

[1] www.nanocyl.be

Table 1
Parameters obtained from mechanical and thermal analyses

	dY/dV_f (GPa)	Y_{Eff} (GPa)	$d\chi/dV_f$	b/R	D (nm)	b (nm)
Arc-MWNT	123 ± 15	329 ± 40	2.26 ± 0.06	0.81 ± 0.01	25 ± 5	10 ± 2
CVD-3	230 ± 154	610 ± 410	5.1 ± 0.3	1.47 ± 0.04	16 ± 5	12 ± 5
CVD-2	361 ± 134	955 ± 355	9.7 ± 0.9	2.27 ± 0.1	14 ± 5	16 ± 6
CVD-1	794 ± 91	2094 ± 240	13.7 ± 0.8	2.83 ± 0.1	15 ± 5	21 ± 8
DWNT	1194 ± 227	3147 ± 600	33.4 ± 11	4.87 ± 0.8	2.5 ± 1	6 ± 3

The effective nanotube stiffness is represented by Y_{Eff}, while b is the thickness of the crystalline coating. R and D are the nanotube radius and diameter, respectively. Nanotube diameters were measured by TEM.

The model most commonly used for the analysis of the Young's modulus of nanotube-reinforced composites is the rule of mixtures (RM) as modified by Cox [13] and Krenchel [14]:

$$Y = (\eta_o Y_{Eff} - Y_P)V_f + Y_P \quad (1)$$

where Y, Y_{Eff} and Y_P, are the composite modulus, the effective nanotube modulus and the polymer modulus. The volume fraction is represented by V_f, while η_o is the fiber orientation efficiency factor [14,15]. This has been shown to be close to $\eta_o = 0.38$ for PVA-nanotube thin films [16]. While other models are available [4], the RM is by far the simplest and most intuitive. This is illustrated by its prediction that the modulus enhancement is simply related to the nanotube modulus by:

$$\frac{dY}{dV_f} = \eta_o Y_{Eff} - Y_P \approx \eta_o Y_{Eff} \quad (2)$$

This shows that for thin films with $\eta_o = 0.38$, the maximum possible modulus enhancement is $dY/dV_f = 380$ GPa (the maximum possible nanotube modulus is ~1 TPa). We can use this model in conjunction with the dY/dV_f values presented in Table 1 to calculate the effective nanotube moduli for the nanotubes used in this study. These data are presented in Table 1. Values for the effective modulus range from 329 GPa for the Arc-MWNT to 3147 GPa for the DWNT. The values for the CVD tubes range from 610 GPa to 2094 GPa. With the exception of the Arc-MWNT samples, all these values are far too high. CVD MWNT are expected to have moduli of much less than 100 GPa [17]. While DWNT can be extremely stiff, their effective modulus is expected to be <1 TPa. In general it is clear that the rule of mixtures significantly underestimates the data found in this study. This is unexpected as the rule of mixtures as presented above is expected to represent an upper bound for the modulus as calculated using the isostrain approximation [18].

In addition, differential scanning calorimetry (DSC) measurements were carried out for all films. For all composites the DSC curves (not shown) were similar in form to those presented in figure 1 of Ref. [7]. A large melt peak was observed at approximately 160–210 °C, indicating the presence of an ordered polymer phase in all samples. This volume fraction of ordered phase, χ, was calculated for all composites and was observed to increase with nanotube content as shown in Fig. 2. This parameter is equivalent to the crystallinity in semi-crystalline polymers. However, we will continue to refer to it as an ordered phase as it is not clear that this phase is a true crystal. This increase in the fraction of ordered polymer can be characterized by the slope ($d\chi/dV_f$) of the $\chi - V_f$ curve measured at low V_f. These values are given in Table 1 with ($d\chi/dV_f$) ranging from 2.26 for the Arc-MWNT composites to 33.4 for the DWNT-based composites.

A linear increase of χ with volume fraction suggests that each nanotube has an ordered polymer coating associated with it in agreement with previous reports [6,8]. These coated nanotubes are in turn embedded in an amorphous matrix. By modeling the ordered coating as a cylindrical shell it can be shown that χ scales with the volume fraction as [8]:

$$\chi = \left(\frac{b^2 + 2Rb}{R^2}\right)V_f + \chi_o \quad (3)$$

where b is the average thickness of the ordered polymer coating, R is the nanotube radius and χ_0 is the contribution from any crystalline/ordered regions not associated with the nanotubes. Fitting Eq. (3) to the data in Fig. 2 allows us to calculate b/R for each nanotube type. These data are presented in Table 1 with b/R varying from 0.81 to 4.87 for the Arc-MWNT and DWNT samples, respectively. The average nanotube diameters as measured from TEM are also given in Table 1. Taking these into account we can see that b varies from approximately 6.1 nm for the DWNT to 21 nm for the CVD-1 samples.

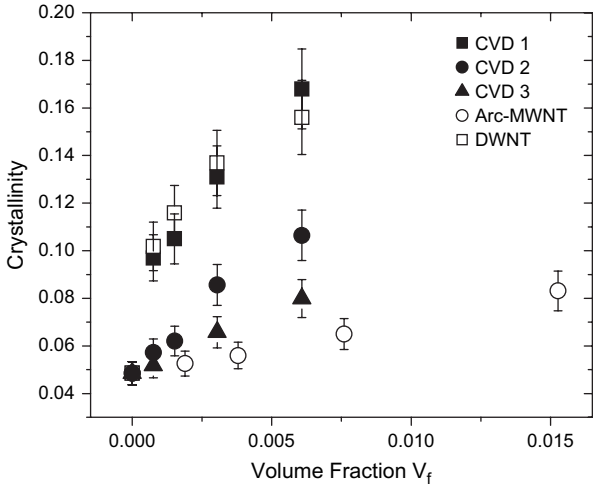

Fig. 2. Polymer crystallinity as a function of nanotube volume fraction for all tube types in PVA matrices.

It should be pointed out that nucleation of crystallinity by carbon nanotubes has been observed previously. In general, this has been observed as nucleation of crystallinity in the presence of nanotubes as composites are cooled from the melt [19–22]. However, microscopic studies on solution processed SWNT–polypropylene composites have demonstrated fibrillar crystallites in an otherwise uniform composite. This suggests the nucleation of a crystalline polymer coating during film drying [19]. Similar effects have been observed for carbon-nanofiber filled polymer composites [21].

While it is clear that the rule of mixtures cannot explain the mechanical results, it appears that the mechanical reinforcement as represented by dY/dV_f scales with both $d\chi/dV_f$ and b/R. This suggests that the enhancement in Young's modulus may be linked to the ordered polymer coating nucleated by the nanotubes. Regions of ordered polymer are known to be both stiffer and stronger than amorphous polymer [18] phases. Thus the roughly cylindrical shell of crystalline polymer associated with each nanotube may act as an extra reinforcing component as suggested by Cadek et al. [5]. In what follows, we modify the standard rule of mixtures to calculate the reinforcing contribution from both the nanotubes and the extra crystalline region.

Besides the nanotube and ordered-polymer phases, an additional region of amorphous polymer embeds the other two in the composite material. When calculating the elastic properties of these composites, one has to account for the contributions from all those three phases. This calls for a generalization of the standard rule of mixtures usually expressed as a weighted average of the elastic moduli of only two constituents [13,14]. Such a generalization can be easily obtained by considering a hybrid structure consisting of a nanotube of radius R coated with an ordered polymer layer of thickness b. This hybrid then enters the standard RM as a single phase with its respective Young's modulus Y_h. Assuming that polymer strands from the amorphous phase are likely to be entangled with others at the edge of the ordered region, we can expect an efficient stress transfer across the interface formed by these two phases. Therefore, for N such hybrid structures of length ℓ dispersed in a volume V, we have for the composite Young's modulus:

$$Y = \left[\frac{N\pi(R+b)^2\ell}{V}\right]Y_h + \left[1 - \frac{N\pi(R+b)^2\ell}{V}\right]Y_a \tag{4}$$

where Y_a is the Young's modulus of the amorphous phase. As the hybrid is itself a composite structure, Y_h should also be expressed as a weighted average, i.e.,

$$Y_h = \frac{R^2}{(R+b)^2}\left[\eta_o Y_{Eff} + \left(\frac{b^2+2Rb}{R^2}\right)Y_\chi\right] \tag{5}$$

where Y_{Eff} and Y_χ are the effective Young's moduli of the nanotube and the crystalline polymer phase, respectively, and the quantity η_o accounts for nanotube orientation effects as described above. Substituting Eq. (5) into Eq. (4) we finally write the composite Young's modulus Y as a three-phase weighted average, hereafter referred to as the double rule of mixtures (DRM),

$$Y = V_f\eta_o Y_{Eff} + (1-V_f)Y_a + \left(\frac{b^2+2Rb}{R^2}\right)V_f(Y_\chi - Y_a) \tag{6}$$

The first two terms in the equation above give the standard RM for nanotubes dispersed in an amorphous polymer matrix. The last term in the equation describes the correction to the composite Young's modulus introduced by the presence of the ordered polymer phase. It is clear that this expression recovers the standard RM for the case in which there is no induced ordering. Whereas it is straightforward to generalize the RM to deal with an arbitrary number of phases, it is worth mentioning that in this case two of our phases have a particular geometry, that is, they are coaxially aligned forming concentric cylindrical layers.

Differentiating the expression above gives:

$$\frac{dY}{dV_f} = \eta_o Y_{Eff} - Y_a + \left(\frac{b^2+2Rb}{R^2}\right)(Y_\chi - Y_a) \tag{7}$$

By inspection of Eq. (3) we can see that

$$\frac{d\chi}{dV_f} = \left(\frac{b^2+2Rb}{R^2}\right) \tag{8}$$

giving

$$\frac{dY}{dV_f} = (Y_\chi - Y_a)\frac{d\chi}{dV_f} + (\eta_o Y_{Eff} - Y_a) \tag{9}$$

This expression clearly shows that, within this framework, dY/dV_f scales linearly with $d\chi/dV_f$. It is worth highlighting that the expression above enables us, not only to calculate the Young's modulus of the composite but also to distinguish between the contribution due to the stress transfer to the nanotube (through Y_{Eff}) and that coming from the crystalline phase. To test this expression, these parameters have been plotted in Fig. 3. A good fit has been found indicating the validity of Eq. (9). We can use the fit parameters to calculate Y_χ and Y_{Eff}. Assuming we can approximate Y_a with the measured polymer modulus ($Y_P = 1.92 \pm 0.33$ GPa) we find $Y_\chi = 46 \pm 5.5$ GPa and $Y_{Eff} = 71 \pm 55$ GPa (taking $\eta_o = 0.38$).

The high modulus of the ordered component is not so surprising. It is well known that while low density polyethylene (PE) has modulus in the 0.1–1 GPa range [18], highly crystalline ultra-high molecular weight PE fibers can have moduli as high as 117 GPa [18]. Thus the presence of ordered polymer regions with modulus of ~46 GPa is reasonable and would be expected to have a significant reinforcing effect.

However, the low value of the effective nanotube modulus, $Y_{Eff} = 71 \pm 55$ GPa, is very surprising. In all cases the nanotubes used in this study are of the order of microns long. This should be long enough to ensure that the effective modulus approaches the true nanotube modulus [4,13,23]. More importantly, while DWNT and Arc-MWNT might be expected to display moduli of the order of 1 TPa [1,24], catalytic nanotubes are expected to have much lower moduli, in the 100 GPa

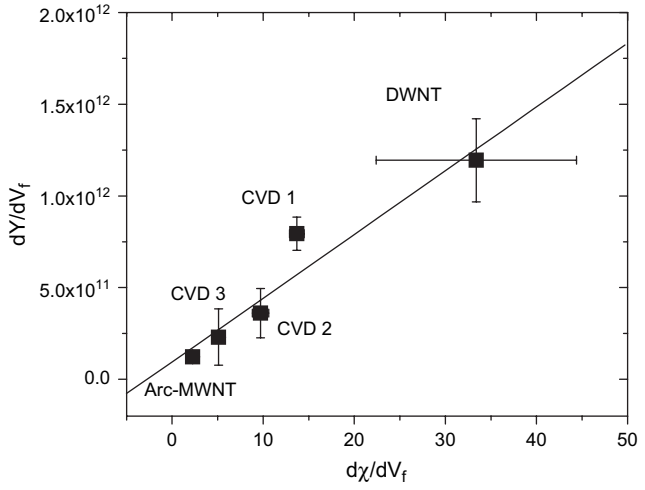

Fig. 3. Rate of increase of modulus with volume fraction plotted against rate of increase of crystallinity with volume fraction for all tube types studied. The solid line is a fit to Eq. (9).

range [17]. Given this large expected variation in moduli, we should not expect to see a straight line at all in Fig. 3. At the very least we might expect the Arc-MWNT and DWNT to sit on a line with a slope defined by the modulus of crystalline polymer but with an intercept appropriate for high modulus nanotubes. Similarly the CVD nanotubes should sit on a line with similar slope but with a much lower intercept, appropriate to their lower moduli.

The fact that we see all the nanotube types on the same line with an intercept appropriate for extremely low modulus nanotubes can only mean that the intrinsic stiffness of the nanotubes plays very little role in the reinforcement mechanism. The primary cause of the reinforcement is the presence of a reasonably stiff ordered polymer phase nucleated at the nanotube surface. This phase is clearly well bound to the amorphous matrix resulting in significant load transfer from amorphous to ordered phase. However, if the nanotubes do not play as large a role as expected, this suggests poor load transfer from ordered phase to nanotube. It is not totally clear why this should be so. One possibility is that, contrary to previous claims by us and others [5,6,8,25,26], an ordered interface does not necessarily lead to good stress transfer. While this is possible, the evidence for high stress transfer in the presence of a crystalline interface is compelling [8,25,26]. In addition this is known to be the case in some polymer–nanofiber composites [27]. More research is required to answer this question. It is possible that some variation on the pull-out experiments carried out by Wagner and co-workers can shed light on this issue [28,29]. Measurements of the polymer–nanotube interfacial shear strength in the presence and absence of thermally nucleated crystallinity would provide a conclusive answer to this problem. However, whatever may be the effect of this ordered polymer/induced crystallinity on interfacial stress transfer, it is clear that the presence of extra nanotube-nucleated polymer ordering can have a significant positive effect on composite mechanical properties.

In conclusion, both Young's modulus and polymer crystallinity were observed to increase linearly with nanotube volume fraction for a range of nanotube types embedded in polyvinyl alcohol. It has been suggested that this increase in crystallinity is due to nucleation of an ordered polymer phase at the nanotube surface. In order to ascertain the effect of this crystallinity on the composite Young's modulus, a simple model based on the rule of mixtures has been developed. This model predicts a linear relationship between dY/dV_f and $d\chi/dV_f$ for polymer–nanotube composites. This relationship has been observed for the samples measured in this study. Fitting the model to the experimental data yields a value for the modulus of the ordered polymer phase of $Y_\chi = 46 \pm 5.5$ GPa. More surprisingly it gives a value for the nanotube effective modulus of $Y_{\mathrm{Eff}} = 71 \pm 55$ GPa. This unexpectedly low value suggests poor polymer–nanotube stress transfer. As a result most of the reinforcement is due to the nucleation of polymer crystallinity by the nanotubes.

Acknowledgements

JNC wishes to thank IRCSET for financial support. MSF thanks SFI for financial support.

References

[1] Wong EW, Sheehan PE, Lieber CM. Nanobeam mechanics: elasticity, strength, and toughness of nanorods and nanotubes. Science 1997;277:1971–5.
[2] Yu M, Lourie O, Dyer MJ, Kelly TF, Ruoff RS. Strength and breaking mechanism of multiwalled carbon nanotubes under tensile load. Science 2000;287:637–40.
[3] Yu MF, Files BS, Arepalli S, Ruoff RS. Tensile loading of ropes of single wall carbon nanotubes and their mechanical properties. Physical Review Letters June 2000;84(24):5552–5.
[4] Tucker CL, Liang E. Stiffness predictions for unidirectional short-fiber composites: review and evaluation. Composites Science and Technology 1999;59(5):655–71.
[5] Cadek M, Coleman JN, Barron V, Hedicke K, Blau WJ. Morphological and mechanical properties of carbon-nanotube-reinforced semicrystalline and amorphous polymer composites. Applied Physics Letters 2002;81(27):5123–5.
[6] Cadek M, Coleman JN, Ryan KP, Nicolosi V, Bister G, Fonseca A, et al. Reinforcement of polymers with carbon nanotubes: the role of nanotube surface area. Nano Letters February 11, 2004;4(2):353–6.
[7] Coleman JN, Blau WJ, Dalton AB, Munoz E, Collins S, Kim BG, et al. Improving the mechanical properties of single-walled carbon nanotube sheets by intercalation of polymeric adhesives. Applied Physics Letters 2003;82(11):1682–4.
[8] Coleman JN, Cadek M, Blake R, Nicolosi V, Ryan KP, Belton C, et al. High performance nanotube-reinforced plastics: understanding the mechanism of strength increase. Advanced Functional Materials 2004;14(8):791–8.
[9] Dalton AB, Collins S, Munoz E, Razal JM, Ebron VH, Ferraris JP, et al. Super-tough carbon-nanotube fibres. Nature 2003;423(6941):703.
[10] Cadek M, Murphy R, McCarthy B, Drury A, Lahr B, Barklie RC, et al. Optimisation of the arc-discharge production of multi-walled carbon nanotubes. Carbon 2002;40(6):923–8.
[11] Delpeux S, Szostak K, Frackowiak E, Bonnamy S, Beguin F. High yield of pure multiwalled carbon nanotubes from the catalytic decomposition of acetylene on in-situ formed cobalt nanoparticles. Journal of Nanoscience and Nanotechnology October 2002;2(5):481–4.

[12] Blond D, Barron V, Ruether M, Ryan KP, Nicolosi V, Blau WJ, et al. Enhancement of modulus, strength and toughness in PMMA based composites by the incorporation of PMMA functionalised nanotubes. Advanced Functional Materials 2006;16(12):1608–14.
[13] Cox HL. The Elasticity and strength of paper and other fibrous materials. British Journal of Applied Physics 1952;3:72–9.
[14] Krenchel H. Fibre reinforcement. Copenhagen: Akademisk Forlag; 1964.
[15] Coleman JN, Khan U, Gun'ko YK. Mechanical reinforcement of polymers using carbon nanotubes. Advanced Materials 2006;18(6):689–706.
[16] Shaffer MSP, Windle AH. Fabrication and characterization of carbon nanotube/poly(vinyl alcohol) composites. Advanced Materials 1999; 11(11):937–41.
[17] Salvetat JP, Kulik AJ, Bonard JM, Briggs GAD, Stockli T, Metenier K, et al. Elastic modulus of ordered and disordered multiwalled carbon nanotubes. Advanced Materials 1999;11(2):161–5.
[18] Callister WD. Materials science and engineering: an introduction. New York: Wiley; 2003.
[19] Assouline E, Lustiger A, Barber AH, Cooper CA, Klein E, Wachtel E, et al. Nucleation ability of multiwall carbon nanotubes in polypropylene composites. Journal of Polymer Science Part B: Polymer Physics 2003; 41(5):520–7.
[20] Grady BP, Pompeo F, Shambaugh RL, Resasco DE. Nucleation of polypropylene crystallization by single-walled carbon nanotubes. Journal of Physical Chemistry B June 13, 2002;106(23):5852–8.
[21] Sandler J, Broza G, Nolte M, Schulte K, Lam YM, Shaffer MSP. Crystallization of carbon nanotube and nanofiber polypropylene composites. Journal of Macromolecular Science Part B: Physics 2003;42(3–4): 479–88.
[22] Xie XL, Aloys K, Zhou XP, Zeng FD. Ultrahigh molecular mass polyethylene/carbon nanotube composites – crystallization and melting properties. Journal of Thermal Analysis and Calorimetry 2003;74(1): 317–23.
[23] Ward IM, Sweeney J. The mechanical properties of solid polymers. London: John Wiley and Sons; 2004.
[24] Salvetat JP, Briggs GAD, Bonard JM, Bacsa RR, Kulik AJ, Stockli T, et al. Elastic and shear moduli of single-walled carbon nanotube ropes. Physical Review Letters February 1, 1999;82(5):944–7.
[25] Frankland SJV, Caglar A, Brenner DW, Griebel M. Molecular simulation of the influence of chemical cross-links on the shear strength of carbon nanotube–polymer interfaces. Journal of Physical Chemistry B March 28, 2002;106(12):3046–8.
[26] Wall A, Coleman JN, Ferreira MS. Physical mechanism for the mechanical reinforcement in nanotube–polymer composite materials. Physical Review B March 25, 2005;71:125421–6.
[27] Wu C-M, Chen M, Karger-Kocsis J. Interfacial shear strength and failure modes in sPP/CF and iPP/CF microcomposites by fragmentation. Polymer 2001;42(1):129–35.
[28] Barber AH, Cohen SR, Kenig S, Wagner HD. Interfacial fracture energy measurements for multi-walled carbon nanotubes pulled from a polymer matrix. Composites Science and Technology 2004;64(15):2283–9.
[29] Barber AH, Cohen SR, Wagner HD. Measurement of carbon nanotube–polymer interfacial strength. Applied Physics Letters 2003;82(23): 4140–2.
[30] Coleman JN, Khan U, Blau WJ, Gun'ko YK. Small but strong: A review of the mechanical properties of carbon nanotube–polymer composites. Carbon 2006;44(9):1624–52.